Environmental Technology & Innovation 17 (2020) 100540

Contents lists available at ScienceDirect

Environmental Technology & Innovation

journal homepage: www.elsevier.com/locate/eti

Facile development of sunlit ZnO nanoparticles-activated carbon hybrid from pernicious weed as an operative nano-adsorbent for removal of methylene blue and chromium from aqueous solution: Extended application in tannery industrial wastewater

M. Kamaraj *, N.R. Srinivasan, Gizachew Assefa, Amare T. Adugna, Muluken Kebede

College of Biological and Chemical Engineering, Addis Ababa Science and Technology University, Addis Ababa 16417, Ethiopia

ARTICLE INFO

Article history:
Received 12 July 2019
Received in revised form 12 November 2019
Accepted 13 November 2019
Available online 16 November 2019

Keywords:
Activated carbon–ZnO
Composite
Tannery waste
Weed management
Eco-friendly
Pollutant removal

ABSTRACT

In this study, zinc oxide nanoparticles (ZnO-NPs) and activated carbon (AC) are produced from parthenium weed plant using a green synthesis technique. ZnO-NPs loaded parthenium weed activated carbon (ZnONPs-PWAC) is used to remove pollutants (Methylene Blue (MB) and Chromium (Cr (VI)) from aqueous solution and also extended to treat with real industrial tannery wastewater. A comprehensive analysis is done with various forms of ZnO based particles (ZnO-NPs, ZnONPs-PWAC) to test its photocatalytic activity. Further, the photocatalytic activity of biosynthesized ZnO-NPs is evaluated by measuring the efficiency of decolorization (>93%) for different dyes (Malachite Green, Congo Red, and Methylene Blue) under sunlight irradiation. The maximum removal (> 99%) of MB is obtained at 60 min by ZnONPs-PWAC and 130 min by PWAC. The maximum equilibrium percentage removal of Cr (VI) is found to be 99% around 90 min for ZnONPs-PWAC and 160 min for PWAC. The enhancement in removal efficiency is due to the combined reaction of photocatalysis and adsorption. The parameters such as pollutant concentration, pH, and the amount of ZnONPs-PWAC are varied to understand its effective removal of MB and Cr (VI) in wastewater. Moreover, the efficiency of ZnONPs-PWAC is found to be more than 92% against industrial tannery wastewater. Overall, ZnONPs-PWAC can be used as an alternative and operative material to remove MB and Cr (VI) in wastewater treatment.

1. Introduction

Water pollution is one of the critical environmental problems worldwide. Wastewater containing dyes and heavy metal ions discharged from various industries induce voluminous mutilation to the ecological system of water bodies (Nasrollahzadeh et al., 2018). The toxic dyes and heavy metals present in wastewater are considered to be harmful to the ecological system due to their chemical stability, difficulty in purification, toxicity, and transport through the trophic

* Correspondence to: Department of Biotechnology, College of Biological and Chemical Engineering, Addis Ababa Science and Technology University, Addis Ababa 16417, Ethiopia.
E-mail address: drkamarajm@gmail.com (M. Kamaraj).

https://doi.org/10.1016/j.eti.2019.100540
2352-1864/

chain (Nagajyoti et al., 2010; Ghaedi et al., 2012a,b). These contaminants create several mutagenic, toxic, teratogenic and carcinogenic effects on aquatic and human life, resulting in several human health disorders such as organ dysfunctions of the kidney, brain, liver, reproductive system, central nervous system and epigenetic alterations even at very low concentration (Ozdes et al., 2010; Bazrafshan et al., 2015).

Chromium (Cr) is one of the heavy metals which mainly exist as Cr (III) and Cr (VI) in a natural environment. Among these, Cr (VI) is more soluble, mobile and toxic. It causes destructive effects on animals and humans than Cr (III) (Modenes et al., 2017). Hexavalent chromium is disposed into the environment by the discharge of wastewater from several industries (leather tanning, textile, cement, steel, metal processing, electroplating, etc.) (Nakkeeran et al., 2018). Particularly, methylene blue (MB) is one of the most frequently used basic dyes in several applications including dyeing of cotton, leather, wool, paper, silk and the production of ink and quality control test of concrete and motor, etc. (Tsai et al., 2009). The contamination of this dye into water bodies causes acute toxic effects to human-like skin irritation, itching, exasperation to the gastrointestinal tract with symptoms of nausea, diarrhea, vomiting, chest pain, severe headache, profuse sweating, methemoglobinemia, dyspnea, and cyanosis, etc. if ingested along with water. It also creates a permanent injury to the human and animal eyes (Bukallah et al., 2007; Ho et al., 2009).

The removal of such bio resilient and toxic pollutants from wastewater can be achieved by various physical and chemical methods like reverse osmosis ozonation, biosorption, membrane filtration, coagulation, adsorption, biodegradation, electrochemical oxidation, adsorption, and photocatalytic degradation, etc. (Ghaedi et al., 2015; Kamaraj et al., 2014). Among them, adsorption and photocatalytic degradation techniques received much attention due to its cost-effective operational process (Chatterjee et al., 2010; Nasrollahzadeh et al., 2018)

Activated carbon (AC) is a low cost and non-toxic material which is considered as an adsorbent for pollutant removal due to its high surface area and porous structure (Sathishkumar et al., 2012). Nanoparticles are the most well-utilized materials in photocatalytic degradation of pollutants that can be more effective when loaded on the surface of activated carbon and receiving much interest in recent years on wastewater treatment (Ghaedi et al., 2013; Roosta et al., 2014; Fu et al., 2015; Khosravi et al., 2018). Zinc Oxide nanoparticles (ZnO-NPs) (n-type semiconductor metal oxide) are drawing interest in a wide range of applications, including photocatalytic degradation due to its non-toxic, effective and inexpensive to produce (Agarwal et al., 2017).

Parthenium hysterophorus L. (Asteraceae family) is selected as a pernicious weed to synthesis activated carbon and ZnO nanoparticles (nano-adsorbent) in this work. Parthenium is an annual herb, aggressive alien weed species and it has been considered as one of the top ten worst noxious weeds of the world and has assumed the status of a significant health hazard (Rajeshwari and Subburam, 2002). In Ethiopia, the colonization efficiency of the weed is much higher than other indigenous plants, resulting in the reduction of cultivable areas of agricultural lands. As of now, there are no sustainable long term management strategies to eradicate this weed (Getachew, 2017). However, the utilization of this weed plant as the source for the preparation of nanoparticle-loaded activated carbon would be an economical and practical approach for environmental cleanup.

In this work, ZnO Nanoparticle loaded parthenium weed activated carbon (ZnONPs-PWAC) is produced by a green waste conversion method for the removal of pollutants from aqueous solution. MB and Cr are used as the model pollutants to determine the adsorption efficiency of ZnONPs-PWAC at different experimental conditions such as pH, nano-adsorbent and adsorbate dose in aqueous solution. Further, Cr removal efficiency of ZnONPs-PWAC is also investigated with industrial wastewater, collected from Ethiopia.

2. Materials and methods

2.1. Chemicals

The chemicals used in this research were analytical reagent grade purchased from different sellers in Ethiopia. Hydrochloric acid and Nitric acid were purchased from Sigma-Aldrich, India. Zinc Nitrate, Zinc Chloride, and Sodium Hydroxide were purchased from HiMedia Pvt Ltd, India. Potassium dichromate, 1, 5 diphenylcarbazide was obtained from Merck, Germany. Congo Red, Malachite Green and Methylene blue were purchased from Titan Biotech Ltd, India.

2.2. Plant material collection, processing, extraction, and analysis

Parthenium weed plant is collected from different fields in and around Addis Ababa Science and Technology University, Ethiopia. Parthenium weed powder (PWP) is prepared from the plant sample after drying under room temperature for 10 days. Aqueous extract of PWP (AEPWP) is prepared by adding 50 g of PWP into 1 L of distilled water and the mixture was further heated for 20 min at 80 °C and filtered. The preliminary qualitative phytochemical analysis of AEPWP is tested according to the method of Harborne (1973).

2.3. Production of parthenium weed activated carbon (PWAC)

Production of PWAC is carried out as described in Murugesan et al. (2019). Briefly, the physical activation of PWP is executed in a muffle furnace (P330, MAALOB, Scientific Equipment Pvt Ltd, Germany) at 400 °C for 2 h. The chemical activation is done by $ZnCl_2$ impregnation with a 1:1 ratio for 2 h at 400 °C. The prepared carbon material is immersed in 1 M HCl for 24 h to leach out the leftover $ZnCl_2$. The material is further washed with distilled water for four times and dehydrated at 80 °C for 6 h.

2.4. Green synthesis of ZnO nanoparticles (ZnO-NPs) using PWP extract

ZnO-NPs synthesis is carried out as described in Murugesan et al. (2019). Briefly, the reaction mixture (60 ml of AEPWP and 140 ml of 1 M Zinc Nitrate hexahydrate [$Zn(NO_3)_2 \cdot 6H_2O$]) is stirred for 2 h at 100 °C until the green precipitation. The supernatant is filtered and agitated further for 2 h at 150 °C until the pale yellow precipitation. The precipitate washed continuously with ethanol and distilled water and annealed for 2 h at 400 °C to get white color powder as resultant material.

2.5. The photocatalytic efficiency of ZnO-NPs under visible light irradiation

Dye solutions such as Congo Red, Malachite Green, and Methylene Blue are subjected to photocatalytic activity of ZnO-NPs. The reaction vessel containing 20 mg of green synthesized ZnO-NPs and 100 ml of dye solutions (10 mg L^{-1} concentration) are kept under sunlight for 5 to 7 h. The percentage of decolorization is measured according to (Kamaraj et al., 2014).

2.6. Preparation of ZnO-nanoparticles loaded parthenium weed activated carbon (ZnONPs-PWAC)

The procedure for the preparation ZnONPs-PWAC is adopted from Ghaedi et al. (2012a,b). 100 mg of ZnO-NPs is added in a beaker containing 100 ml distilled water and stirred using a magnetic stirrer for 30 min at 200 rpm and then ultrasonicated for 2 h. After that, 5 g PWAC is added and sonicated for 2 h and then stirred under magnetic stirrer for 12 h at 200 rpm. After the deposition of ZnONPs on PWAC, the mixture is filtered using centrifugation at 8000 rpm for 10 min. The filtrate ZnONPs-PWAC is dried in a hot air oven for 8 h at 200 °C and then stored at room temperature for further use.

2.7. Characterization of ZnO-NPs, PWAC, and ZnONPs-PWAC

Fourier Transform Infrared (FTIR) spectrophotometer (USA) is used to examine the functional groups. X-ray diffraction (XRD) studies are carried out to examine the crystallographic edifice of materials using D8 Advanced XRD, Bruker. The surface morphology of the materials is investigated using a scanning electron microscope (SEM) (Model JSM 6390LV). Microporosity area, external surface area, total porosity area, Brunauer–Emmett–Teller (BET) theory of surface area characteristics of PWAC and ZnONPs-PWAC were analyzed using standard methodology (Rajeshwari et al., 2010). The pH drift method is used to calculate the pH of point zero charges (pH_{PZC}) (Lopez-Ramon et al., 1999).

2.8. Pollutant removal efficiency comparison of PWAC and ZnONPs-PWAC

Stock solution (1000 mg L^{-1}) for Cr (VI) and MB is prepared and then diluted to various other concentrations of working solutions. The pH is varied by the addition of 0.1 M of HCl/NaOH solutions. Now, 50 mg of PWAC and ZnONPs-PWAC were introduced to a 250 ml glass beaker containing 100 ml solution of MB (100 mg L^{-1}/pH-6) and Cr (VI) (20 mg L^{-1}/pH-2). The experiment is performed under both sunlight and dark condition to compare the efficiency of ZnONPs-PWAC with PWAC. After exposure, the supernatant solution is separated using a centrifuge, operated at 6000 rpm for 10 min. The residual Cr (VI) is analyzed by complexing with acidified 1,5 diphenylcarbazide (Klimaviciute et al., 2010). Then, the concentration of the remaining quantity in the filtrate is measured by monitoring its absorbance value at 670 nm for MB (Kamaraj and Umamaheswari, 2017) and 540 nm for Cr (VI) (Elwakeel, 2010). The pollutant removal percentage (% R) of PWAC and ZnONPs-PWAC is calculated based on the optical density values (Kamaraj and Umamaheswari, 2017). The pollutant removal trials are performed in triplicates to measure mean and the standard deviations are expressed as error bars.

2.9. Effect of different operating variables on Cr (VI) and MB removal by ZnONPs-PWAC

The different operating variables such as ZnONPs-PWAC dosage, pH and adsorbate (Cr (VI) and MB) concentration are tested to determine the efficiency of ZnONPs-PWAC under visible light (sunlight) exposure. The adsorbate dosage is investigated over a range of 20–200 mg L^{-1}. The amount of nano-adsorbent (ZnONPs-PWAC) is varied from 10–100 mg to evaluate the experimental condition. The effect of different pH of the solution with the performance of nano-adsorbent is tested by varying the pH range from 2–10.

2.10. ZnONPs-PWAC performance efficiency on real tannery industrial wastewater (TIWW)

To understand its potential against industrial wastewater, three samples were collected from different tannery industries, located near Kality industrial area, Addis Ababa, Ethiopia. The collected samples are filtered through a filter paper (Whatman No 42, Maidstone, England) and labeled as TIWW1, TIWW2, and TIWW3. The efficiency of ZnONPs-PWAC on tannery industry wastewater has been studied in a batch experiment setup as follows: tannery industry wastewater-100 ml; ZnONPs-PWAC dosage- 100 mg; contact time- 5 h, pH of the solution-3 and stirring speed of 250 rpm. The physicochemical parameters such as pH, Chemical Oxygen Demand (COD), Total Dissolved Solids (TDS), Biological Oxygen Demand (BOD), Sulfate (So_4^{2-}) and Cr (VI) are measured before and after treatment with ZnONPs-PWAC according to the standard procedures (APHA, 2005).

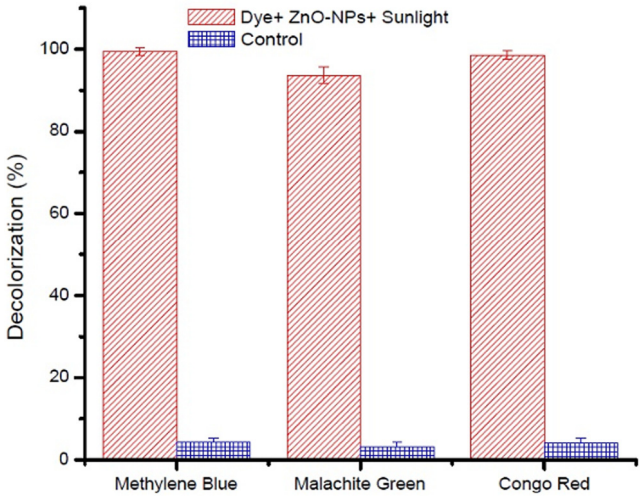

Fig. 1. Photocatalytic decolorization efficiency (%) of ZnO-NPs on selective dyes under sunlight irradiation.

3. Results and discussion

3.1. Phytochemical screening

Since the synthesis process involves AEPWP, phytochemical screening is carried out to find out the phytoconstituents in the sample. It is found that Carbohydrate, Protein, Alkaloid, flavonoids, Steroids, Glycosides, Catechins, Terpenoids, Phenolic groups, and Tannins are present in the sample, but Anthraquinones are absent. The functional groups of phytochemicals in the extract facilitate the reduction of the process of metals, and subsequently form the numbers of nanoparticles with controlled particle size and shape (Mohamad et al., 2014). The presence of the metal-reducing compound in PWP indicates that the PWP could be utilized to synthesize nanoparticles, thus converting this noxious weed into a valuable product (Hasna et al., 2017).

3.2. The photocatalytic efficiency of ZnO-NPs

The photocatalytic activity of biosynthesized ZnO-NPs is carried out under sunlight between 8 am to 4 pm since the fluctuations in solar intensity are less during the period (Nagaraja et al., 2012). The decolorization percentage of different dyes is found to be 93, 98 and 99 for Malachite Green, Congo Red, and Methylene Blue, respectively (Fig. 1). Light intensity and electron–hole formation in the photochemical reaction are responsible for initiating the rate of photocatalysis (Cassano and Alfano, 2000). The present study emphasizes an economical photo dynamism (sunlight) to overcome the problems associated with other light sources like mercury light tungsten light, and UV source which are costly and lethal (Kamaraj et al., 2014)

3.3. Characterization of ZnO-NPs, PWAC, and ZnONPs-PWAC

3.3.1. XRD analysis

XRD pattern of ZnO-NPs (Fig. 2a) confirms the hexagonal phase structure of synthesized crystalline ZnO (Lupan et al., 2008) and the average particle size is found to be in the range of 22–35 nm using Scherrer formula. The peaks at 23.89° and 45.00° correspond to (002) and (001) planes (Fig. 2b) of the disordered graphite form, which is similar to activated carbon (Das et al., 2015). The other peaks are in good agreement with the standard data of Joint Committee on Powder Diffraction Standards (ZnO- JPDS No.36–1451; C- JCPDS-82-1691) (Eskizeybek et al., 2012; Sulistianti et al., 2017). The XRD pattern of the ZnONPs-PWAC (Fig. 2c) shows the additional characteristic peaks of ZnO-NPs along with assigned carbon planes. It indicates that the amorphous structure of activated carbon changes into some degree of crystalline nature (Altintig and Kirkil, 2016). This is due to the addition of ZnO-NPs on the surface of PWAC.

3.3.2. SEM analysis

The morphology of prepared ZnO-NPs, PWAC and ZnONPs-PWACs is analyzed using SEM. As seen in Fig. 3a, ZnO-NPs exhibit different shapes such as hexagonal and spherical, and it can be attributed due to the effect of the metal-reducing capacity of PWP extract. These particles possess an average size below 25 to 95 nm, and it is found to be arbitrary, inconsistent and aggregated/clustered forms. This is in good agreement with previously reported work (Rajiv et al., 2013).

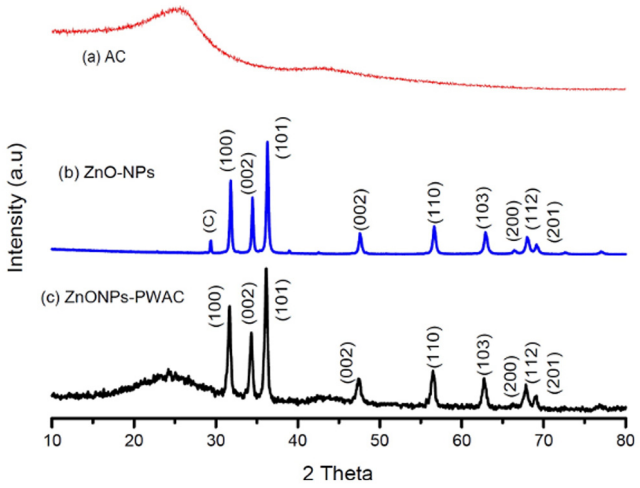

Fig. 2. XRD analysis of PWAC (a), ZnO-NPs, (b) and ZnONPs-PWAC (c).

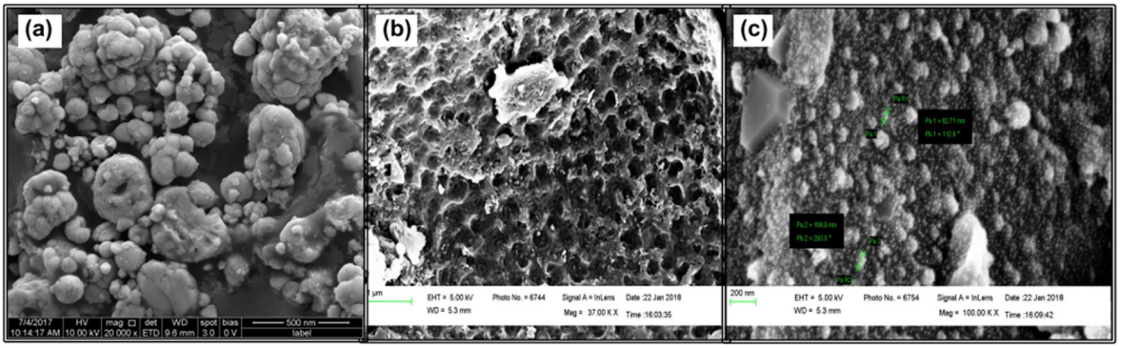

Fig. 3. SEM analysis of ZnO-NPs (a), PWAC (b) and ZnONPs-PWAC (c).

The densification of agglomeration may create a narrow space between the particles for uniform distribution of oxidized metal anions in the 3-D polymeric network structure (Sangeetha et al., 2011). SEM analysis of PWAC (Fig. 3b) shows that the morphology contains many various sizes of holes and caves, which may be due to ZnCl2 evaporation during the carbonization step (Rajeshwari et al., 2010). The porous nature of activated carbon may provide a more possibility of additional loading space for ZnO-NPs. Fig. 3c shows many white spots distributed over the surface of PWAC, confirming the presence of ZnO-NPs on the external surface of PWAC. Even though some of the pores of PWAC are occupied by ZnO-NPs, the sample still exhibits a porous nature with a relatively large pore volume (Muthirulan et al., 2013). The addition of ZnO-NPs on PWAC is increases the more active site and surface area of the nano-adsorbent, which improves the adsorption efficiency of the contaminants (Liu et al., 2017).

3.3.3. FTIR analysis

The characteristic functional groups of the materials are investigated using FTIR spectral analysis. As seen in Fig. 4b, the peaks observed in the region between 600–400 cm^{-1} is due to Zn-O vibrations of ZnO-NPs (Tas et al., 2000). The peak at 3375 cm^{-1} is due to free NH stretching vibrations and peaks at 1395 cm^{-1}, and 1533 cm^{-1} are due to N–H bending mode. The peak at 1600 cm^{-1} confirms the primary amines, whereas the peak at 2245 cm^{-1} indicates the presence of alkyls (C≡C stretch) and nitriles (C≡N stretch) vibrations. These results confirm the presence of certain plant compounds, which are responsible for the reduction, capping and stability of the ZnO-NPs (Datta et al., 2017; Sindhura et al., 2013).

From Fig. 4c, the presence of organic components in PWP (Fig. 4a) is disappeared after performing carbonization. The peaks at 864 cm^{-1} and 1434 cm^{-1} indicates the presence of group C–O–H and C=C, respectively. The peak broadening around 1552–1664 cm^{-1} is probably caused by the formation of C–O formation, which coincides with the C=C (Chafidz et al., 2018). ZnONPs-PWAC (Fig. 4d) shows some more peaks at 864 and 1434, 1637 cm^{-1}, which are similar to PWAC. The peaks at 3749, 2379, 1086, 400–500 cm^{-1} are apparent when ZnO-NPs join PWAC via the loading process (Altintig and Kirkil, 2016).

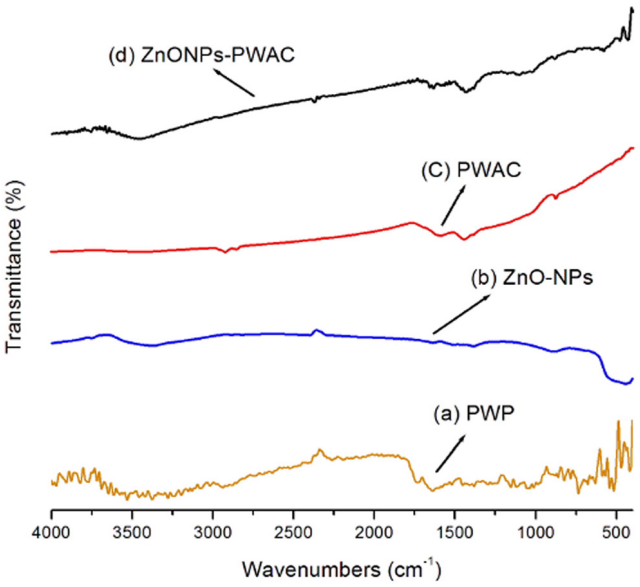

Fig. 4. FT-IR analysis of PWP (a), ZnO-NPs (b), PWAC (c) and ZnONPs-PWAC (d).

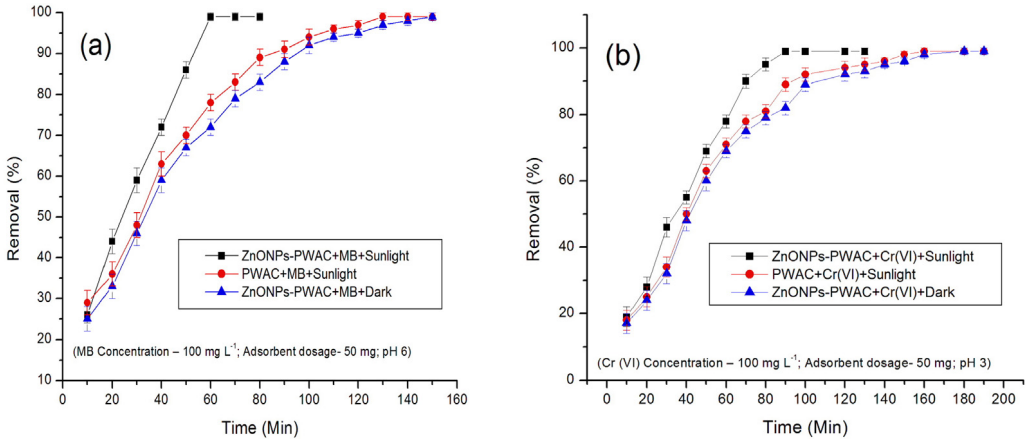

Fig. 5. MB (a) and Cr (VI) (b) removal efficiency comparison of PWAC and ZnONPs-PWAC.

3.3.4. Characteristics of surface area, porosity area, and pH_{PZC}:

The values of the BET Surface area (m^2/g), microporosity area (m^2/g), external surface area (m^2/g), total porosity area (cm^2/g) and microporosity volume (cm^3/g) of the PWAC are identified as 1089.2, 604.4, 318.78, 0.71 and 0.51 respectively, for the PWAC and 890.9, 454.3, 259.12, 0.59 and 0.47, respectively, for ZnONPs-PWAC (Table 1). The values of ZnONPs-PWAC are lesser than the values of PWAC due to the addition of ZnO-NPs on the surface of carbon, leading to pore blockage. The specific surface area of the ZnO-NPs is lower than the AC, which attributes to the lower surface area to ZnONPs-PWAC than PWAC (Han et al., 2011). In the case of pHPZC, the values are almost similar for PWAC (6.9) and ZnONPs-PWAC (6.8).

3.4. Efficiency comparison of PWAC and ZnONPs-PWAC

MB (100 mg L^{-1}/pH 6) and Cr (VI) (20 mg L^{-1}/pH 3) are selected as the model pollutant to compare the improved efficiency of ZnONPs-PWAC with PWAC on the removal of the contaminant from aqueous solution (Fig. 5). This experiment is performed for 4 h under sunlight with an amount of 50 mg. As seen in Fig. 5, ZnONPs-PWAC gives higher pollutant removal efficiency than PWAC under sunlight irradiation. The maximum removal equilibrium (>99%) of MB is attained at 60 min by ZnONPs-PWAC and 130 min by PWAC (Fig. 5a). For Cr (VI), the maximum removal equilibrium percentage (> 99%) is obtained around 90 min for ZnONPs-PWAC and 160 min for PWAC (Fig. 5b). It shows that the efficiency of ZnONPs-PWAC is improved as the equilibrium time decreased almost half of the time taken for PWAC. The higher percentage of

Table 1
Characteristics of textural properties of PWAC and ZnONPs-PWAC.

S.No	Parameters	PWAC	ZnONPs-PWAC
1	BET surface area (m^2/g)	1089.2	890.9
2	Microporosity area (m^2/g)	604.4	454.3
3	External surface area (m^2/g)	318.75	259.12
4	Total porosity area (cm^3/g)	0.71	0.59
5	Microporosity volume (cm^3/g)	0.51	0.47
6	pH_{PZC}	6.9	6.8

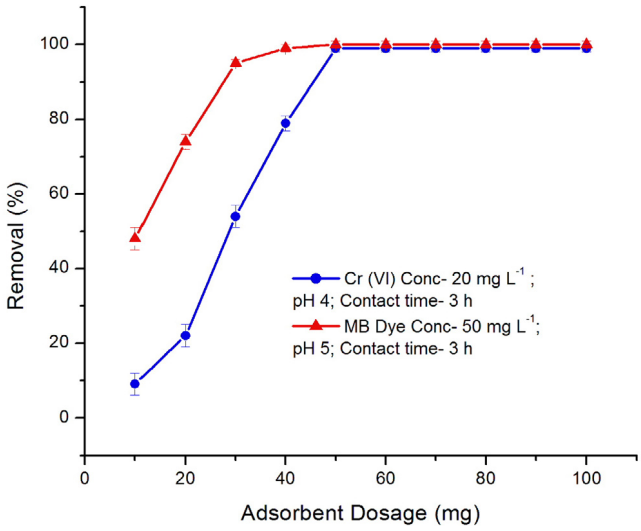

Fig. 6. Effect of ZnONPs-PWAC dosage on removal of MB and Cr (VI) from aqueous solution.

removal for ZnONPs-PWAC could be attributed to the interaction between the particle and pollutant through ion-dipole, or hydrogen bonding of pollutant molecule and the photocatalytic properties may get altered by the addition of ZnO-NPs functional groups onto PWAC (Ghaedi et al., 2012a,b). This result shows that the removal rate percentage for both MB and Cr (VI) is increased rapidly for ZnONPs-PWAC, as compared to PWAC.

The experiment is carried out under light and dark condition to identify the difference in the removal efficiency of both materials (Fig. 5). The removal efficiency is found to be higher (>99%) under light irradiation, as compared to the dark condition. However, effective behavior is more perceptible when the concentration of pollutants is lower than the initial concentration. For both test pollutants, the rapid reduction of concentration in the first stage is due to the adsorption reaction between adsorbate and adsorbent. The removal is higher for ZnONPs-PWAC than PWAC due to the combined reaction of photocatalysis and adsorption. The adsorption leads to the reduction of test molecule concentration in an aqueous solution that allows the light source to reach the surface of the ZnONPs-PWAC, which triggers the photocatalytic mechanism of ZnO-NPs loaded on the surface of the carbon.

The maximum removal percentage is recorded around 150 min for MB and 180 min for Cr (VI) treated by ZnONPs-PWAC under dark condition, which is lesser than PWAC (130 min for MB and 160 min for Cr (VI). The removal efficiency of ZnONPs-PWAC is delayed in a smaller extent than PWAC under dark condition. This is due to the surface area and porosity values of ZnONPs-PWAC, which are lesser than the PWAC (Cruz et al., 2017). Mesopores of AC is vital for the absorption of organic compounds from the suspension (Hadoun et al., 2013). When ZnO-NPs are loaded, the porosity characteristics are altered to less extent and cause a small decrease in microporosity volume. The efficiency reduces under dark condition as there is no light to activate the photocatalytic mechanism of the ZnO-NPs that make them inactive. This is in good agreement with previous literature (Cruz et al., 2017; Altintig and Kirkil, 2016; Kakavandi et al., 2014; Zhao et al., 2013). Overall, ZnONPs-PWAC has improved and better Cr (VI) and MB removal efficiency than PWAC. The impregnation of ZnO-NPs enhances the removal of a cationic dye and heavy metals in the aqueous phase.

3.5. Effect of nano-adsorbent dosage

The experiment is performed in a batch mode to ascertain the effect of ZnONPs-PWAC on the removal of selected model pollutant from aqueous solution using the fixed conditions for MB (100 mg L^{-1}/pH 6/3 h) and Cr (VI) (20 mg L^{-1}/pH 3/3 h) with various amounts of ZnONPs-PWAC (10–100 mg). It shows that the removal rate is increased from 9% to 99% for Cr (VI) and 48% to 99% for MB with the increment of ZnONPs-PWAC from 10 to 100 mg (Fig. 6). Moreover, the percentage

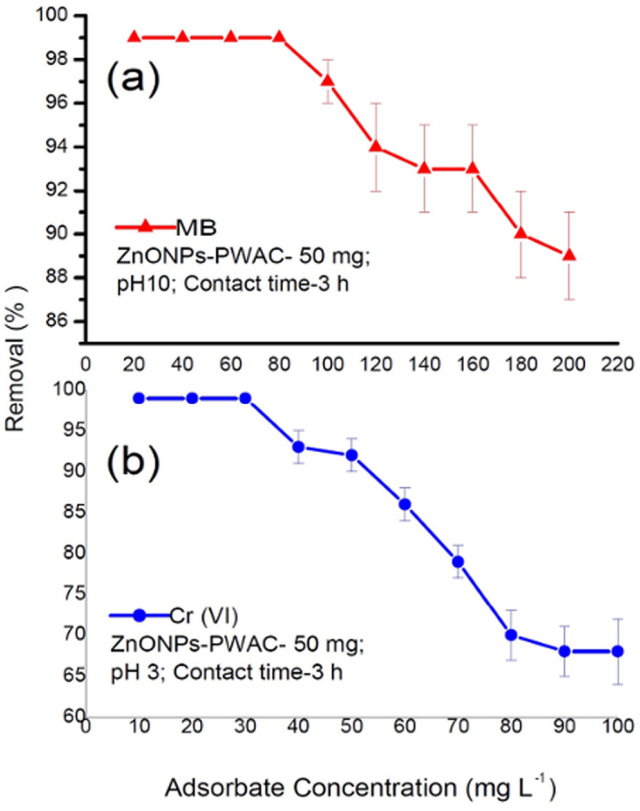

Fig. 7. Effect of MB (a) and Cr (VI) (b) concentration on removal efficiency of ZnONPs-PWAC.

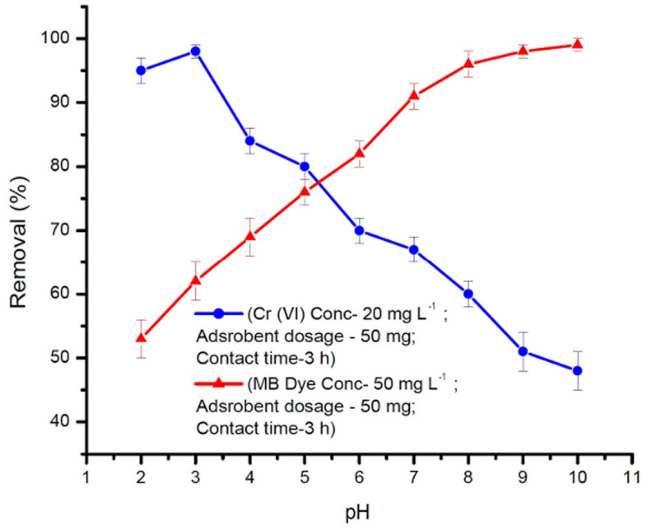

Fig. 8. Effect of solution pH on removal of MB and Cr (VI) from aqueous solution.

of removal is increased with increment in adsorbent, which probably due to the increase in the availability of active sites and surface area on the ZnONPs-PWAC (Jung et al., 2013). The maximum removal equilibrium is obtained for MB at 40 mg and Cr (VI) at 50 mg of nano-adsorbent. Further, the increase in adsorbent levels does not bring any significant changes in the removal as the pollutant reaches a saturation level (Kakavandi et al., 2014). This is in good agreement with previous studies on the removal of MB (Ghaedi et al., 2015) and Cr (VI) from aqueous solution (Enniya et al., 2018).

3.6. Effect of pollutant concentration

The experiments are performed with variable initial concentration for MB (20–200 mg L^{-1}/pH 6) and Cr (VI) (10–100 mg L^{-1}/pH 3) with a fixed condition like ZnONPs-PWAC dose of 50 mg and a contact time of 3 h to investigate the dependence of removal efficiency of ZnONPs-PWAC on substrate concentration. The initial concentration of adsorbate molecules provides a vital driving force to sweep overall mass transfer resistance between the aqueous and solid phases (Ho et al., 2005; Dogan et al., 2004). As seen in Fig. 7, the percentage of removal decreased from 99 to 89% for MB and 99 to 68% for Cr (VI). This is due to the further increase in the initial concentration of test pollutant (MB and Cr (VI)). The excess pollutant concentration leads to a decrease in the removal percentage probability due to the saturation and limitation of ZnONPs-PWACs active surface. When the concentration of target pollutant increase, more and more of those molecules get adsorbed on the surface of the adsorbent and make it unavailable to react with remaining target molecules (Ahmed et al., 2011).

3.7. Effect of solution pH

To check the effect of solution pH on the removal of MB and Cr (VI) from aqueous solutions by ZnONPs-PWAC, the experiment is performed at different pH values ranging from 2 to 10. The other parameters are fixed as follows: initial concentration of test sample - 20 mg L^{-1} for Cr (VI) and 20 mg L^{-1} for MB; dosage of ZnONPs-PWAC- 50 mg; contact time - 3 h. The obtained results are depicted in Fig. 8. The maximum removal percentage of >98% is observed at pH 2.0 and 6.0 for Cr (VI) and MB, respectively. In the case of Cr (VI), the removal efficiency is decreased with increasing the pH from 3.0 to 10.0 as >98 to 48%. The exception is observed at extreme acidic pH (∼2), the difference in Cr existing form and profusion amount of H+ ions may block the active sites of ZnONPs-PWAC, leading to lower removal efficiency. For MB removal, the removal efficiency is increased from 53 to 99% with increasing pH from 2.0 to 10.0.

The removal efficiency of ZnONPs-PWAC is attributed based on the solution pH, which influences the sorption affinity by either altering the ionic forms of the test solution adsorbent or the surface properties (Attia et al., 2010). The pH of the solution affects the removal process by different functioning pathways such as structural changes, changes in charge of both adsorbate and adsorbent (Ghaedi et al., 2015). The removal of test pollutants (MB and Cr (VI)) by ZnONPs-PWAC can be conveyed by electrostatic interaction and chemical reaction.

Chromium exists in two forms at acidic pH: as chromic acid (H_2CrO_4) in the pH range of 1–2 and as hydrogen chromate ions ($HCrO_4^-$) in the pH range of 3–7 (Sakulthaew et al., 2017). Particularly, ZnONPs-PWAC surface protonated by hydrogen ions at strong acidic conditions, and it leads to the positively charged surface and favors the electrostatic attraction between Cr (VI) as in the form of $HCrO_4^-$ (Garg et al., 2007; Demiral et al., 2008). Cr (VI) removal efficiency of ZnONPs-PWAC is decreased at an alkaline condition due to the existence of Cr (VI) in the form of chromate ions (CrO_4^{2-}), which is rivalry with the hydroxide ions presented on the sorbent surface (Karthikeyan et al., 2005; Parlayici et al., 2015). This explanation supports the high Cr (VI) adsorption capacity at acidic pH (3), and it is subsequently reduced by increasing pH values due to the gradual conversion of CrO_4^{2-} and $Cr_2O_7^{2-}$ ions (Garg et al., 2007; Enniya et al., 2018). The tendency of active sites in the adsorbent attaches to the reactive centers of MB is triggered by the increasing solution pH of MB, resulting in high removal efficiency at pH 10. The pKa values of MB molecule is 3.8 and increasing the pH from acidic to alkaline, leading to electrostatic interaction attraction force, thereby increasing the dye removal (Dogan et al., 2004).

The variation in the removal of Cr (VI) and MB depends on the initial pH of the test solution. The surface of ZnONPs-PWAC may get a positive charge at lower pH (<5) due to the presence of H_3O^+ ions (Baccar et al., 2009; Asfaram et al., 2014), leading electrostatic attraction between Cr (VI) and electrostatic repulsion between MB molecules. In contrast, the surface of ZnONPs-PWAC is negatively charged at higher pH (>5) which is ascribed due to the weakened protonation degree of carbon surface with the predominance of OH^-ions and deprotonation of anionic oxygen functional groups (Li et al., 2008). The negatively charged ZnONPs-PWAC in the test solution disperses Cr (VI) homogeneously via electrostatic repulsion (Hu et al., 2013), but also enrich electrostatic attraction with the cationic MB molecules (Ramesha et al., 2011; Peng et al., 2016).

3.8. Efficiency of ZnONPs-PWAC on tannery industry wastewater treatment

The treatment of industrial wastewater is a challenging task because it has different micropollutants, which influence the effect of adsorbent used for the treatment. Further testing has been expanded to check the efficiency of ZnONPs-PWAC on real tannery industry wastewater where the micropollutants are diverse in nature. The physicochemical parameters such as COD, TDS, BOD, So_4^{2-} and Cr (VI) are measured in a homogenized wastewater sample before and after treatment with ZnONPs-PWAC, as shown in Table 2 (average value of triplicates). The removal efficiency (%) is measured around 92,91,92,93,98 (TIWW1), 89,90,91,92,99 (TIWW2) and 91,91,92,93,98 (TIWW2) for the parameters of COD, TDS, BOD, So_4^{2-} and Cr (VI), respectively. Swathi et al. (2014) reported the reduction of COD, BOD, and Cr (VI) are found to be 68%, 73%, and 79.9% respectively in tannery water treated with rice husk as an adsorbent. The reduction percentage is found to be 81, 91, 86, 93 and 88 for COD, TDS, BOD, So_4^{2-} and Cr (VI), respectively, for the tannery wastewater treated with rice husk silica powder (Sivakumar, 2015). The reduction rate found in the present study is comparatively more than the previous studies (Sivakumar, 2015; Swathi et al., 2014). The validated optimum result from the study indicates that the efficiency of ZnONPs-PWAC on real tannery industry wastewater and it can also be extended to the other type of industrial wastewater. Further investigations are required to test the material efficiency in column experiments on multiple wastewater effluents with different organic and inorganic contaminants.

Table 2
Efficiency of ZnONPs-PWAC on tannery industry wastewater treatment.

Parameters (mg L^{-1})	TIWW 1			TIWW 2			TIWW 3		
	Raw	Treated	Removal treatment efficiency (%)	Raw	Treated	Removal treatment efficiency (%)	Raw	Treated	Removal treatment efficiency (%)
COD	5950	425	92.85714	6540	680	89.60245	6120	520	91.50327
TDS	3195	260	91.86228	3657	330	90.97621	3270	290	91.1315
BOD	1900	138	92.73684	2000	165	91.75	1940	140	92.78351
Sulfate	159	12	92.45283	182	13	92.85714	173	11	93.64162
Cr (VI)	69.25	0.81	98.83032	73.79	0.25	99.6612	70.12	0.98	98.6024

4. Conclusion

The composite material (ZnONPs-PWAC) is successfully developed by loading ZnO-NPs on the surface of AC. AC is prepared from an abundant noxious weed Parthenium, collected from Ethiopia. The synthesized materials are characterized by SEM, XRD, FTIR and BET analysis for better understanding their nature. The photocatalytic activity of green synthesized ZnO-NPs is tested on selected dyes and found to be dominant. The new nano-adsorbent (ZnONPs-PWAC) developed has applied to remove MB and Cr (VI) from aqueous solution. Experiments that combine adsorption and photocatalysis are carried out with, and without sunlight irradiation. It reveals that the ZnONPs-PWAC has improved and better Cr (VI) and MB removal efficiency than that of PWAC. The optimum adsorbent, dosage (mg), adsorbate concentration (mg L^{-1}) and pH for ZnONPs-PWAC are obtained as 40, 80, 10 (MB) and 50,30,3 (Cr (VI)), respectively. The efficiency of ZnONPs-PWAC is further tested in three tannery industrial wastewater. It is observed that the percentage of reduction is more than 90% on the parameters such as COD, TDS, BOD, So_4^{2-} and Cr (VI). From the analysis, ZnONPs-PWAC has many advantages like high surface area, combined mechanism, high pollutant removal capacity, adequate sensitivity, productivity, simple synthesis, and cost-effective.

Declaration of competing interest

The authors declare that they have no known competing financial interests or personal relationships that could have appeared to influence the work reported in this paper.

Acknowledgments

The authors are grateful to Addis Ababa Science and Technology University, Ethiopia for the funding (Internal Research Grant Reference No-AASTU-IRG 12/09) and laboratory services for this research work.

References

Agarwal, H., Venkatkumar, S., Rajeshkumar, S., 2017. A review on green synthesis of zinc oxide nanoparticles –An eco-friendly approach. Res. Effic. Tech. 3, 406–413.
Ahmed, S., Rasul, M.G., Martens, W.N., Brown, R., Hashib, M.A., 2011. Advances in heterogeneous photocatalytic degradation of phenols and dyes in wastewater: A review. Water Air Soil Poll. 215, 1–35.
Altintig, E., Kirkil, S., 2016. Preparation and properties of ag-coated activated carbon nanocomposites produced from wild chestnut shell by $ZnCl_2$ activation. J. Taiwan Inst. Chem. Eng. 63, 180–188.
APHA-AWWA-WPCF, 2005. Standard Methods for the Examination of Water and Wastewater, 20th ed. American Public Health Association, Washington, D. C. New York.
Asfaram, A., Fathi, M.R., Khodadoust, S., Naraki, M., 2014. Removal of Direct Red 12B by garlic peel as a cheap adsorbent:Kinetics, thermodynamic and equilibrium isotherms study of removal. Spectrochim. Acta. A Mol. Biomol. Spectrosc. 127, 415–421.
Attia, A.A., Khedr, S.A., Elkholy, S.A., 2010. Adsorption of chromium ion (VI) by acid activated carbon. Braz. J. Chem. Eng. 27, 183–193.
Baccar, R., Bouzid, J., Feki, M., Montiel, A., 2009. Preparation of activated carbon from Tunisian olive-waste cakes and its application for adsorption of heavy metal ions. J. Hazard. Mater. 162, 1522–1529.
Bazrafshan, A.A., Hajati, S., Ghaedi, M., 2015. Synthesis of regenerable $Zn(OH)_2$ nanoparticle loaded activated carbon for the ultrasound assisted removal of malachite green: optimization, isotherm and kinetics. RSC Adv. 5, 79119–79128.
Bukallah, S.B., Rauf, M.A., AlAli, S.S., 2007. Removal of methylene blue from aqueous solution by adsorption on sand. Dyes Pigm. 74, 85–87.
Cassano, A.E., Alfano, O.M., 2000. Reaction engineering of suspended solid hetereogenous photocatalytic reactors. Catal. Today 58, 167–197.
Chafidz, A., Astuti, W., Augustia, V., Novira, D.T., Rofiah, N., 2018. Removal of methyl violet dye via adsorption using activated carbon prepared from randu sawdust (*Ceiba pentandra*). IOP Conf. Ser: Earth Environ. Sci. 167, 012013.
Chatterjee, D., Patnam, V.R., Sikdar, A., Moulik, S.K., 2010. Removal of some common textile dyes from aqueous solution using fly ash. J. Chem. Eng. Data 55, 5653–5657.
Cruz, G.J.F., Gómez, M.M., Solis, J.L., Rimaycuna, J., Solis, R.L., Cruz, J.F., Rathnayake, B., Keiski, R.L., 2017. Composites of ZnO nanoparticles and biomass based activated carbon: adsorption, photocatalytic and antibacterial capacities. Water Sci. Technol. 2, 492–508.
Das, D., Samal, D.P., Meikap, B.C., 2015. Preparation of activated carbon from green coconut shell and its characterization. J. Chem. Eng. Process. Technol. 6, 1–7.
Datta, A., Patra, C., Bharadwaj, H., Kaur, S., Dimri, N., et al., 2017. Green synthesis of zinc oxide nanoparticles using *Parthenium hysterophorus* leaf extract and evaluation of their antibacterial properties. J. Biotechnol. Biomater. 7 (271).

Demiral, H., Demiral, I., Tümsek, F., Karabacakoglu, B., 2008. Adsorption of chromium (VI) from aqueous solution by activated carbon derived from olive bagasse and applicability of different adsorption models. Chem. Eng. J. 144, 88–196.
Dogan, M., Alkan, M., Tu¨rkyılmaz, A., Ozdemir, Y., 2004. Kinetics and mechanism of removal of methylene blue by adsorption onto perlite. J. Hazard. Mater. 109, 141–148.
Elwakeel, K.Z., 2010. Removal of Cr(VI) from alkaline aqueous solutions using chemically modified magnetic chitosan resins. Desalination 250, 105–112.
Enniya, I., Rghioui, L., Jourani, A., 2018. Adsorption of hexavalent chromium in aqueous solution on activated carbon prepared from apple peels. Sustain. Chem. Pharm. 7, 9–16.
Eskizeybek, V., Sari, F., Gulce, H., Gulce, A., Avci, A., 2012. Preparation of the new polyaniline/ZnO nanocomposite and its photocatalytic activity for degradation of methylene blue and malachite green dyes under UV and natural sun lights irradiations. Appl. Catal. B. Environ. 119-120, 197–206.
Fu, X., Yang, H., Lu, G., Tu, Y., Wu, J., 2015. Improved performance of surface functionalized TiO_2 /activated carbon for adsorption-photocatalytic reduction of Cr(VI) in aqueous solution. Mater. Sci. Semicond. Process. 39, 362–370.
Garg, U.K., Kaur, M.P., Garg, V.K., Sud, D., 2007. Removal of hexavalent chromium from aqueous solution by agricultural waste biomass. J. Hazard. Mater. 140, 60–68.
Getachew, M., 2017. Threats and management options of parthenium (*Parthenium hysterophorus l.*) in ethiopia. Agri. Res. Tech. Open Access J. 10, 555798.
Ghaedi, M., Heidarpour, S.H., Kokhdan, S.N., Sahraie, R., Daneshfar, A., Brazesh, B., 2012b. Comparison of silver and palladium nanoparticles loaded on activated carbon for efficient removal of Methylene blue: Kinetic and isotherm study of removal process. Powder Technol. 228, 18–25.
Ghaedi, M., Khajesharifi, H., Yadkuri, A.M., Roosta, M., Sahraei, R., Daneshfar, A., 2012a. Cadmium hydroxide nanowire loaded on activated carbon as efficient adsorbent for removal of romocresol green. Spectrochim. Acta. A. Mol. Biomol. Spectrosc. 86, 62–68.
Ghaedi, M., Nasab, A.G., Khodadoust, S., Sahraei, R., Daneshfar, A., 2015. Characterization of zinc oxide nanorods loaded on activated carbon as cheap and efficient adsorbent for removal of methylene blue. J. Ind. Eng. Chem. 21, 986–993.
Ghaedi, M., Niknam, K., Zamani, S., Larki, H.A., Roosta, M., Soylak, M., 2013. Silica chemically bonded N-propyl kriptofix 21 and 22 with immobilized palladium nanoparticles for solid phase extraction and preconcentration of some metal ions. Mater. Sci. Eng. C. 33, 3180–3189.
Hadoun, H., Sadaoui, Z., Souami, N., Sahel, D., Toumert, I., 2013. Characterization of meso- porous carbon prepared from date stems by H_3PO_4 chemical activation. Appl. Surf. Sci. 280, 1–7.
Han, T.Y., Worsley, M.A., Baumann, T.F., Satcher, Jr., J.H., 2011. Synthesis of ZnO coated activated carbon aerogel by simple sol–gel route. J. Mater. Chem. 21, 330–333.
Harborne, J.B., 1973. Phytochemical Methods. Chapman and Hall Ltd, London, pp. 49–188.
Hasna, A.S., Rajeshwari, S., Kamaraj, M., Venckatesh, R., 2017. Photocatalytic potential of ZnO/TiO2-a bio-nanocomposite from *Ocimum basilicum* l. var. purpurascens benth.-LAMIACEAE. Bioinspir. Biomim. Nan. 5, 85–90.
Ho, Y.S., Chiang, T.H., Hsueh, Y.M., 2005. Removal of basic dye from aqueous solution using tree fern as a biosorbent. Process. Biochem. 40, 119–124.
Ho, Y.S., Malarvizhi, R., Sulochana, N., 2009. Equilibrium isotherm studies of methylene blue adsorption onto activated carbon prepared from *Delonix regia* pods. J. Environ. Protect. Sci. 3, 111–116.
Hu, X., Yu, Y., Hou, W., Zhou, J., Song, L., 2013. Effects of particle size and pH value on the hydrophilicity of graphene oxide. Appl. Surf. Sci. 273, 118–121.
Jung, C., Heo, J., Han, J., Her, N., Lee, S.J., Oh, J., Ryu, J., Yoon, Y., 2013. Hexavalent chromium removal by various adsorbents: powdered activated carbon, chitosan, and single/multi-walled carbon nanotubes. Sep. Purif. Technol. 106, 63–71.
Kakavandi, B., Kalantary, R.R., Farzadkia, M., Mahvi, A.H., Esrafili, A., Azari, A., Yari, A.R., Javid, A.B., 2014. Enhanced chromium (VI) removal using activated carbon modified by zero valent iron and silver bimetallic nanoparticles. J. Environ. Health. Sci. Eng. 12, 1–10.
Kamaraj, M., Ranjith, K.S., Rajeshwari, S., Rajendrakumar, R.T., Hasna, A.S., 2014. Photocatalytic degradation of endocrine disruptor Bisphenol-A in the presence of prepared $Ce_xZn_{1-x}O$ nano composites under sunlight irradiation. J. Environ. Sci. 26, 2362–2368.
Kamaraj, M., Umamaheswari, P., 2017. Preparation and characterization of Groundnut shell activated carbon as an efficient adsorbent for the removal of Methylene blue dye from aqueous solution with microbiostatic activity. J. Mater. Environ. Sci. 8, 2019–2025.
Karthikeyan, T., Rajgopal, S., Miranda, L.R., 2005. Chromium (VI) adsorption from aqueous solution by *Hevea brasilinesis* sawdust activated carbon. J. Hazard. Mater. 124, 192–199.
Khosravi, R., Moussavi, G., Ghaneian, M.T., Ehrampoush, M.H., Barikbin, B., Ebrahimi, A.A., Sharifzadeh, G., 2018. Chromium adsorption from aqueous solution using novel green nanocomposite: Adsorbent characterization, isotherm, kinetic and thermodynamic investigation. J. Mol. Liq. 256, 163–174.
Klimaviciute, R., Bendoraitiene, J., Rutkaite, R., Zemaitaitis, A., 2010. Adsorption of hexavalent chromium on cationic cross-linked starches of different botanic origins. J. Hazard. Mater. 181, 624–632.
Li, D., Mueller, M.B., Gilje, S., Kaner, R.B., Wallace, G.G., 2008. Processable aqueous dispersions of graphene nanosheets. Nat. Nanotechnol. 3, 101–105.
Liu, S., Xu, W.H., Liu, Y.G., Tan, X.F., Zeng, G.M., et al., 2017. Facile synthesis of Cu (II) impregnated biochar with enhanced adsorption activity for the removal of doxycycline hydrochloride from water. Sci. Total Environ. 592, 546–553.
Lopez-Ramon, M.V., Stoeckli, F., Moreno-Castilla, C., Carrasco-Marina, F., 1999. On the characterization of acidic and basic surface sites on carbons by various techniques. Carbon 37, 1215–1221.
Lupan, O., Chow, L., Chao, G., Heinrich, H., 2008. Fabrication and characterization of Zn–ZnO core–shell microspheres from nanorods. Chem. Phys. Lett. 465, 249–253.
Modenes, A.N., de Oliveira, A.P., Espinoza-Quinones, F.R., Trigueros, D.E.G., Kroumov, A.D., Bergamasco, R., 2017. Study of the involved sorption mechanisms of Cr (VI) and Cr (III) species onto dried *Salvinia auriculata* biomass. Chemosphere 172, 373–383.
Mohamad, N.A.N., Arham, N.A., Jai, J., Hadi, A., 2014. Plant extract as reducing agent in synthesis of metallic nanoparticles: Review. Adv. Mater. Res. 832, 350–355.
Murugesan, K., Tareke, K., Gezehegn, M., et al., 2019. Rapid development of activated carbon and ZnO nanoparticles via green waste conversion using avocado fruit peel powder and its high performance efficiency in aqueous dye removal application. J. Inorg. Organomet. Polym. 29, 1368–1374.
Muthirulan, P., Meenakshisundararam, M., Kannan, N., 2013. Beneficial role of ZnO photocatalyst supported with porous activated carbon for the mineralization of alizarin cyanin green dye in aqueous solution. J. Adv. Res. 4, 479–484.
Nagajyoti, P.C., Lee, K.D., Sreekanth, T.V.M., 2010. Heavy metals, occurrence and toxicity for plants: a review. Environ. Chem. Lett. 8, 199–216.
Nagaraja, R., Nagaraju, K., Girija, C.R., Nagabhushana, B.M., 2012. Photocatalytic degradation of Rhodamine B dye under UV/solar light using ZnO nanopowder synthesized by solution combustion route. Powder Technol. 215–216, 91–97.
Nakkeeran, E., Patrab, C., Shahnazb, T., Rangabhashiyam, S., Selvaraju, S.N., 2018. Continuous biosorption assessment for the removal of hexavalent chromium from aqueous solutions using *Strychnos nux* vomica fruit shell. Bioresour. Technol. Rep. 3, 256–260.
Nasrollahzadeh, M.S., Hadavifar, M., Ghasemi, S.S., Chamjangali, M.A., 2018. Synthesis of ZnO nanostructure using activated carbon for photocatalytic degradation of methyl orange from aqueous solutions. Appl. Water Sci. 8, 1–12.
Ozdes, D., Gundogdu, A., Duran, C., Senturk, H.B., 2010. Evaluation of adsorption characteristics of malachite green onto almond shell (*Prunus dulcis*). Sep. Sci. Technol. 45, 2076–2085.

Parlayici, S., Eskizeybek, V., Avc, A., Pehlivan, E., 2015. Removal of chromium (VI) using activated carbon-supported-functionalized carbon nanotubes. J. Nanostruct. Chem. 5, 255–263.
Peng, W., Li, H., Liu, Y., Song, S., 2016. Adsorption of methylene blue on graphene oxide prepared from amorphous graphite: Effects of pH and foreign ions. J. Mol. Liq. 221, 82–87.
Rajeshwari, S., Subburam, V., 2002. Activated parthenium carbon as an adsorbent for the removal of dyes and heavy metal ions from aqueous solution. Bioresour. Technol. 85, 205–206.
Rajeshwari, S., Vevckatesh, R., Gowri, Sangeetha, G., 2010. Activated carbon prepared from eichornia crassipes as an adsorbent for the removal of dyes from aqueous solution. Int. J. Eng. Sci. Technol. 2, 2418–2427.
Rajiv, P., Rajeshwari, S., Venckatesh, R., 2013. Bio-fabrication of zinc oxide nanoparticles using leaf extract of *Parthenium hysterophorus* L. and its size-dependent antifungal activity against plant fungal pathogens. Spectrochim. Acta. A Mol. Biomol. Spectrosc. 112, 384–387.
Ramesha, G.K., Kumara, A.V., Muralidhara, H.B., Sampath, S., 2011. Graphene and graphene oxide as effective adsorbents toward anionic and cationic dyes. J. Colloid. Interf. Sci. 361, 270–277.
Roosta, M., Ghaedi, M., Daneshfar, A., Sahraei, R., Asghari, A., 2014. Optimization of the ultrasonic assisted removal of methylene blue by gold nanoparticles loaded on activated carbon using experimental design methodology. Ultrason. Sonochem. 21, 242–252.
Sakulthaew, C., Chokejaroenrat, C., Poapolathep, A., Satapanajaru, T., Poapolathep, S., 2017. Hexavalent chromium adsorption from aqueous solution using carbon nano-onions (CNOs). Chemosphere 184, 1168–1174.
Sangeetha, G., Rajeshwari, S., Venckatesh, R., 2011. Green synthesis of zinc oxide nanoparticles by aloe *barbadensis miller* leaf extract: Structure and optical properties. Mater. Res. Bull. 46, 2560–2566.
Sathishkumar, P., Arulkumar, M., Palvannan, T., 2012. Utilization of agro-industrial waste *Jatropha curcas* pods as an activated carbon for the adsorption of reactive dye Remazol Brilliant Blue R (RBBR). J. Clean. Prod. 22, 67–75.
Sindhura, K.S., Prasad, T.N.V.K.V., Selvam, P.P., Hussain, O.M., 2013. Synthesis, characterization and evaluation of effect of phytogenic zinc nanoparticles on soil exo-enzymes. Appl. Nanosci. 1, 1–9.
Sivakumar, D., 2015. Hexavalent chromium removal in a tannery industry wastewater using rice husk silica. Global J. Environ. Sci. Manage. 1, 27–40.
Sulistianti, I., Krisnandi, Y.K., Moenandar, I., 2017. Study of CO_2 adsorption capacity of mesoporous carbon and activated carbon modified by triethylenetetramine (TETA). IOP Conf. Series Mater. Sci. Eng. 012041, 1–6.
Swathi, M., Sathya Singh, A., Aravind, S., Ashi Sudhakar, P.K., Gobinath, R., Saranya Devi, D., 2014. Adsorption studies on tannery wastewater using rice husk. Sch. J. Eng. Tech. 2, 253–257.
Tas, A.C., Majewski, P.J., Aldinger, F., 2000. Chemical preparation of pure and strontium- and/or magnesium-doped lanthanum gallate powders. J. Am. Ceram. Soc. 83, 2954–2960.
Tsai, W.T., Chen, H.R., Kuo, K.C., Lai, C.Y., Su, T.C., Chang, Y.M., Yang, J.M., 2009. The adsorption of methylene blue from aqueous solution using waste aquacultural shell powders. J. Environ. Eng. Manage. 19, 165–172.
Zhao, Y., Wang, Z., Zhao, X., Li, W., Liu, S., 2013. Antibacterial action of silver–doped activated carbon prepared by vacuum impregnation. Appl. Surf. Sci. 266, 67–72.